Cancellation of klystron-induced energy and arrival-time variations in linear accelerators with arc-type bunch compressors

Erik Mansten,* Robin Svärd, Sara Thorin, Mikael Eriksson, and Pedro Fernandes Tavares
MAX IV Laboratory, Lund University, Fotongatan 2, 224 84, Lund, Sweden

(Received 20 June 2023; revised 28 February 2024; accepted 21 March 2024; published 24 April 2024)

We explain how the accelerating field amplitude and phase vary with modulator voltage in pulsed radio frequency high-power amplifiers based on klystron tubes. Changes in modulator voltage give rise to correlated changes of amplitude and phase, affecting the properties of the accelerated beam, in particular energy, arrival time, and bunch duration. We show, both theoretically and experimentally, that there exists a postcrest acceleration phase (the *magic angle*) where the changes of beam energy due to phase and amplitude shifts caused by modulator-voltage variations cancel out. When accelerating at the magic angle, the klystron modulator voltage jitter no longer contributes to energy and arrival-time jitter in the accelerator. Off-crest operation at the magic angle can be implemented for bunch compression schemes in accelerators with arc-type bunch compressors, which have positive momentum compaction. The experimental results, obtained at the MAX IV laboratory, show the benefit of operating close to the magic angle in arc-type bunch compressors. In a direct measurement of normalized electron-energy jitter, the energy jitter was reduced by a factor of 1.8 down to 8.2×10^{-5} when operating at the magic angle.

DOI: 10.1103/PhysRevAccelBeams.27.040401

I. INTRODUCTION

Linear accelerators used to drive free-electron lasers (FELs) have already shown the capacity to produce short electron bunches, down to sub-fs bunch duration [1]. At best, the arrival time jitter at full energy is 1 order of magnitude higher than the shortest produced bunches [2–5]. To make use of a short electron bunch duration in time-resolved experiments, the arrival time of the FEL light relative to a pump laser must be measured shot-by-shot and data sorted according to the arrival time [6,7]. A direct consequence of the arrival time jitter is that only a small fraction of the electron bunches arrives during the relevant time window for the experiments. This significantly reduces the effective repetition rate [8].

Advanced synchronization and radio frequency (rf) distribution systems have been designed to minimize energy and timing jitter [8–10]. High demands on klystron modulator voltage stability were also defined with the same goal [2]. Improved energy stability provides direct benefits on the wavelength stability of the produced photons in the following FEL.

To correctly model how klystron modulator voltage affects electron beam energy stability, a correlation of amplitude and phase in klystron tubes [11,12] must be considered. Assuming noncorrelated amplitude and phase jitter can underestimate the calculated energy jitter for acceleration phases precrest and overestimate the jitter for postcrest acceleration. A consequence of the correlation is that there exists an off-crest accelerating phase where the energy and arrival time of the electron bunch become insensitive to modulator high voltage (HV) jitter [11,12].

Electron energy and timing are connected through the momentum compaction in bunch compressors (BCs) [13],

$$\Delta t = \frac{R_{56}}{c}\frac{\Delta E}{E}, \tag{1}$$

where R_{56} is the first-order momentum compaction and c is the speed of light. Magnetic bunch compressors can be divided into chicane and arclike types. Chicane types have negative momentum compaction ($R_{56} \leq 0$). In chicanes, electron bunches are compressed in precrest acceleration schemes. Arc types have positive momentum compaction ($R_{56} \geq 0$) and compress postcrest accelerated bunches [14].

In this work, we provide a theoretical background to the contribution from klystron modulator voltage to variations of the accelerating field amplitude and phase, which in turn affect the electron beam energy and arrival time. The theoretical description includes the off-crest accelerating phase, the *magic angle*, where the electron bunch energy and arrival time are insensitive to modulator HV

*erik.mansten@maxiv.lu.se

fluctuations [11,12]. Compression of the electron bunch at the magic angle is only possible in bunch compressors with positive R_{56}. The arc-type bunch compressors in the MAX IV linac provide a unique opportunity to fully integrate stable operation at the magic angle in the self-linearizing bunch compression scheme. The theoretical predictions are supported by experimental results including accelerating phase and amplitude dependence on modulator voltage as well as a verification of the magic angle. A direct measurement of relative energy jitter shows almost a twofold improvement in energy jitter when operating at the magic angle.

II. AMPLITUDE AND PHASE JITTER IN KLYSTRON TUBES

Klystron tubes are used to amplify rf signals in all high-energy linear accelerators working in the S to X frequency bands. The working principle of klystrons can be found in Ref. [15]. Ensuring that the klystrons operate in saturation with respect to the input rf power, the main contribution to field amplitude jitter is the accelerating HV jitter in the tube. As described below, the output field phase also varies with the HV in correlation with the output amplitude.

The pulsed HV applied between the cathode and anode in the klystron tube is produced by a modulator, based on soft or hard tube circuits [16], thyratrons, or solid-state technology [17]. The HV jitter is in the 0.1% range for thyratrons and other vacuum tubes [18]. Feed-forward circuits have been developed to reduce the thyratron HV jitter [19]. In the latest technology solid-state modulators, the jitter can be as low as 0.001% [2].

Using analytical formalism, one can show that the effect of variations in HV, U_{HV}, is twofold [20] (1) changed output power from the klystron, $P_{\mathrm{rf}} \propto U_{\mathrm{HV}}^{5/2}$, corresponding to a field amplitude change, $A_{\mathrm{rf}} \propto U_{\mathrm{HV}}^{5/4}$ and (2) a phase shift of the rf output due to the altered time of flight through the klystron drift space, $\theta_{\mathrm{rf}} \propto U_{\mathrm{HV}}^{-1/2}$. For simplicity, the phase variation, described above in point 2, assumes a nonrelativistic electron beam inside the klystron tube. The relativistic corrections can be found in [20]. When accelerating off-crest, the correlated amplitude and phase change described above give rise to a combined shift in electron beam energy.

The contributions to amplitude and phase jitter originating from modulator high voltage jitter are correlated and they add up constructively if accelerating precrest or destructively if accelerating postcrest. Consequently, independent treatment of the phase and amplitude underestimates the calculated energy and timing jitter for precrest acceleration and overestimates the jitter for postcrest acceleration. Furthermore, there is a postcrest phase (the magic angle, θ_{magic}) where the two effects cancel out, and the energy and timing of the electron beam become insensitive to modulator HV changes [11,12].

III. MAGIC ANGLE

The energy gain, E_g, of an electron passing an accelerating structure with a phase angle θ relative to the accelerating field can be expressed as

$$E_g(A;\theta) = A\,\cos(\theta), \tag{2}$$

where A is the amplitude of the accelerating voltage. The relative energy shift caused by small amplitude and phase deviations can be calculated by taking the derivative of Eq. (2) with respect to A and θ and normalizing by E_g. The result is

$$\frac{\Delta E_g}{E_g} \approx \frac{\Delta A}{A} - \Delta\theta\,\tan(\theta). \tag{3}$$

We introduce the constants α and β to describe how output amplitude and phase depend on the HV in the klystron,

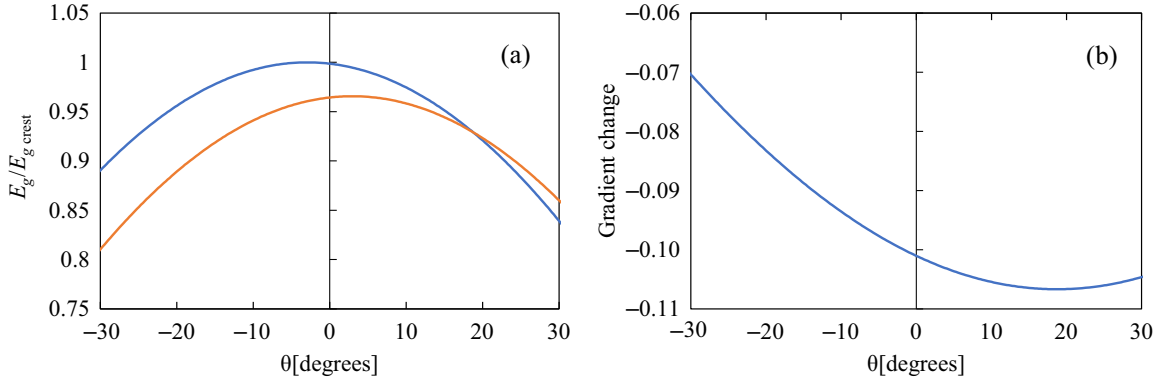

FIG. 1. Illustrations based on analytical calculations. (a) The relative energy gain variation for the nominal HV (blue curve) and for 1% lower HV (red curve). Both curves are normalized with respect to the crest energy for nominal HV. The curves intersect at a phase of 18.5°. (b) The difference between the gradient of the two curves in (a), i.e., the relative gradient change for a 1% difference in HV.

$$\frac{\Delta A}{A} = \alpha \frac{\Delta U_{\mathrm{HV}}}{U_{\mathrm{HV}}}, \tag{4}$$

$$\Delta\theta = \beta \frac{\Delta U_{\mathrm{HV}}}{U_{\mathrm{HV}}}. \tag{5}$$

The parameters α and β are klystron specific and can be retrieved from data sheets, measured data, or analytical calculations. Inserting the expressions from Eqs. (4) and (5) into Eq. (3) gives

$$\frac{\Delta E_g}{E_g} \approx \alpha \frac{\Delta U_{\mathrm{HV}}}{U_{\mathrm{HV}}} - \beta \frac{\Delta U_{\mathrm{HV}}}{U_{\mathrm{HV}}} \tan(\theta). \tag{6}$$

For an accelerating phase

$$\theta_{\mathrm{magic}} = \arctan\left(\frac{\alpha}{\beta}\right), \tag{7}$$

the energy gain variations due to HV changes cancel out. In Fig. 1(a), the energy gain is plotted as a function of phase for two HV settings. We used measured values for one of the MAXIV linac klystrons, $\alpha = 3.4$ and $\beta = 10.3$ rad, to calculate the energy gain. A description of the measurement setup can be found in Sec. V. The magic angle is the intersection point between the red and blue curves in Fig. 1(a).

IV. GRADIENT AND COMPRESSION

By comparing the gradient of the blue and red curves in Fig. 1(a), it is evident that the gradient also varies with HV. The expected gradient jitter contribution from HV jitter can be calculated in the following way:

$$\frac{dE_g}{dt}(\theta, \Delta U_{\mathrm{HV}}) = \frac{\frac{dE_g}{dt}(\theta, \delta U_{\mathrm{HV}}) - \frac{dE_g}{dt}(\theta, 0)}{\delta U_{\mathrm{HV}}} \Delta U_{\mathrm{HV}}, \tag{8}$$

where θ is the bunch phase, δU_{HV} is the small normalized HV difference used for the discrete derivative, and ΔU_{HV} is the expected normalized modulator HV change or jitter. The gradient sensitivity to HV changes is illustrated in Fig. 1(b). The figure shows the difference in gradient of the two curves in Fig. 1(a). Since the derivative is done with respect to angle in radians, a scaling with the angular frequency ω is needed to calculate the energy chirp rate with respect to time.

The ratio of the pulse durations C_{comp} before and after a bunch compressor depends on the energy gain gradient at the bunch phase angle and R_{56} [21].

$$C_{\mathrm{comp}} = \frac{1}{1 + \frac{dE_g}{dt}\frac{R_{56}}{E_g c}}. \tag{9}$$

HV-induced gradient jitter will thus introduce bunch length jitter.

V. EXPERIMENTAL RESULTS

A. rf phase and amplitude measurements

We have conducted direct amplitude and phase measurements at the output of one klystron in the MAX IV linac [22,23]. The measurements provide the coefficients α and β, introduced in Eqs. (4) and (5). The amplitude of the E-field was measured with a directional coupler [24] and the phase was measured by mixing the klystron output with the low-level signal feeding the klystron preamplifier.

In Fig. 2(a), the measured amplitude (blue markers) and phase (red markers) are plotted, while the klystron HV was changed in steps of 1 V. Each data point is averaged over 200 shots. The constants for amplitude (α) and phase (β) changes can be extracted from the derivatives in Fig. 2(a). The dashed lines show the linear fits to the measured data points.

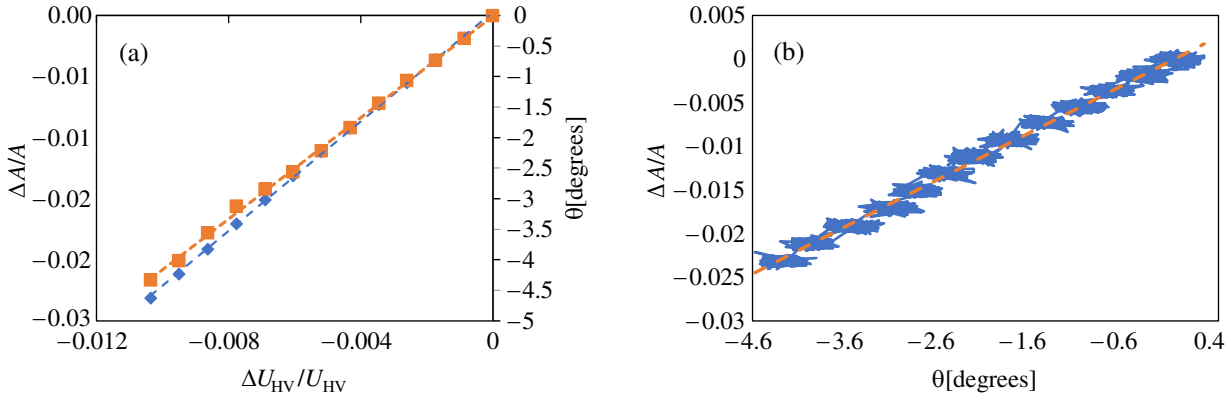

FIG. 2. (a) Averaged amplitude and phase data plotted for a nominal HV setting of 1160V. During the measurement, the HV settings were changed as described in Sec. V B. Amplitude data are plotted in blue, and phase is plotted in red. The marker sizes indicate the vertical standard deviation of the raw data. (b) Scatterplot representation of the same data, where each blue point corresponds to the measured amplitude and phase for one rf pulse. The dashed red line is a linear fit to the data points.

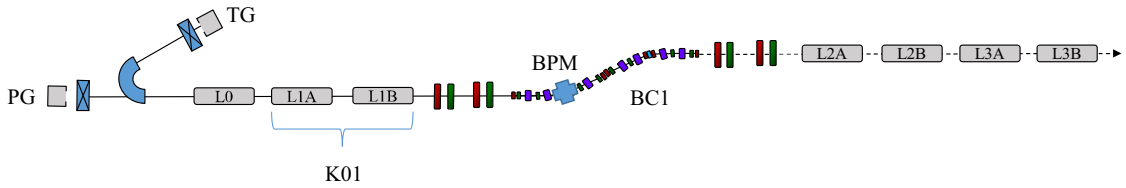

FIG. 3. Photocathode gun (PG) electron bunches are accelerated up to ∼100 MeV electron energy in the first linac (L_{00}). In the following accelerating structure pair L_{01A} and L_{01B}, the beam is further accelerated up to a nominal energy of 250 MeV. In the measurement described in Sec. V B, the rf phase was varied and the sensitivity of energy to modulator high voltage was measured. For each phase, the K01 modulator high voltage was varied between 1180 and 1168 V, and the beam energy variations were recorded with the first BPM at maximum dispersion in BC1.

For a nominal HV of 1160 V, the derivatives give $\alpha = 2.2$ and $\beta = 7.2$ rad. Increasing the nominal HV to 1180 V gives $\alpha = 3.4$ and $\beta = 10.3$ rad.

In Fig. 2(b), the correlation of amplitude and phase is verified by a scatterplot. Each blue data point corresponds to one rf pulse during which amplitude and phase were measured. A linear fit to the data is plotted in dashed red. The slope of the plot in Fig. 2(b) gives the ratio $\alpha/\beta = 0.0054$, corresponding to $\theta_{\text{magic}} = 17.2°$, that is, the magic angle is 1.3° closer to crest for an HV of 1160 V, compared to 1180 V.

Our measured amplitude variations show a higher order dependence on voltage compared to the analytically derived expression in Sec. II ($A_{\text{rf}} \propto {U_{\text{HV}}}^{\alpha}$, $\alpha_{\text{analytical}} = 5/4 < \alpha_{\text{measured}}$).

B. HV sensitivity

In this section, we demonstrate the HV jitter compensation described in Sec. III. We varied the rf phase to klystron K01, θ_{K01}, see illustration in Fig. 3. At each phase setting, the electron beam energy was varied through a change in modulator HV. The energy was measured with a beam position monitor (BPM) in the first dispersive maximum in the following bunch compressor 1 (BC1). The electron energy difference between two modulator HV settings, nominal (1180 V) and nominal minus 12 V, was calculated for each phase. The relative energy difference,

$$\frac{\Delta E_g(\theta)}{E_g(\theta)} = \frac{E_{U_{\text{HV}}=1180\,\text{V}}(\theta) - E_{U_{\text{HV}}=1168\,\text{V}}(\theta)}{E_{U_{\text{HV}}=1180\,\text{V}}(\theta)}, \quad (10)$$

is plotted in Fig. 4. The results show that the electron beam energy is insensitive to HV changes at the magic angle of 18.5°. As a comparison, the measured relative energy shift at −18.5° is 0.07.

Figure 4 also shows in dashed red the calculated relative energy shift given by Eq. (6) for a voltage change of $dU_{\text{HV}}/U_{\text{HV}} = 1\%$. The values for $\alpha = 3.4$ and $\beta = 10.3$ rad were experimentally retrieved, see Sec. V A.

A linear fit (thin dotted blue) of the experimental data can be used to retrieve $\alpha = 3.4$ from the crossing with the y axis and $\beta = 9.9$ rad from the slope. There is good agreement among all our independent measurements of α and β.

The expected contribution of a given modulator voltage jitter to the electron beam energy jitter can be calculated by scaling the data in Fig. 4. The energy jitter corresponding to $dU_{\text{HV}}/U_{\text{HV}} = 2 \times 10^{-5}$ is thus a factor of 500 lower than what is shown in the figure.

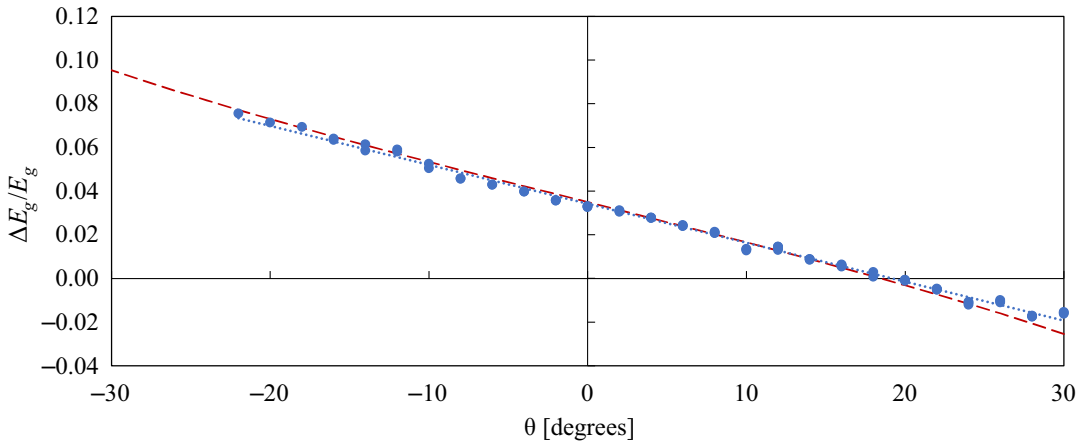

FIG. 4. Normalized energy shift as a function of rf phase, when varying K01 modulator high voltage between 1180 and 1168 V. Measured data plotted with blue dots, linear fit to measured data plotted with a thin dotted line, and calculated values using Eq. (6) are plotted with a red dashed line.

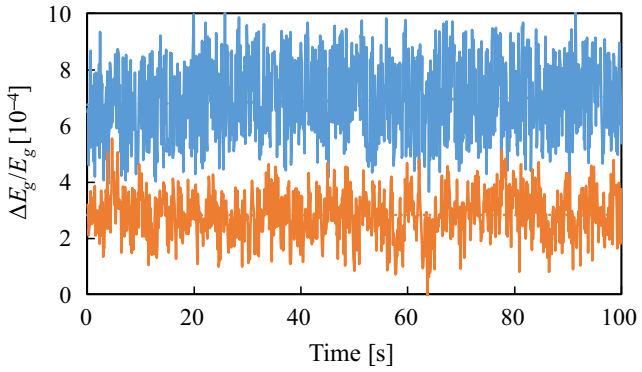

FIG. 5. Measured normalized energy jitter operating K01 at two phases, $\theta = \theta_{\text{magic}}$ is plotted in red and $\theta = -\theta_{\text{magic}}$ is plotted in blue.

C. Beam energy stability

The result of a direct measurement of energy jitter in BC1 is plotted in Fig. 5. The same experimental setup that was presented in Fig. 3 was used for the measurement. The low-level rf (LLRF) feeding all rf stations along the linac was generated from the photocathode gun (PG) laser oscillator via direct conversion using a fast photodiode. The LLRF was amplified in several steps up to kW peak power to feed the klystrons in saturation. More information on the rf system can be found in Refs. [25] and [26]. A conservative assumption that all position jitter measured by the BPM can be attributed to energy jitter has been made.

Electron energy data were acquired for two-phase settings of klystron K01. At the first phase setting, $\theta = \theta_{\text{magic}}$, HV jitter in K01 does not contribute to the energy jitter. Normalized electron energy data for $\theta = \theta_{\text{magic}}$ is plotted in red. The measured rms energy jitter dE_g/E_g of 8.2×10^{-5} is caused by sources other than modulator HV. The jitter can be explained by 0.015° rms phase jitter caused by the direct rf conversion, phase noise in the LLRF amplifiers, or effects in the gun that was not operating at the magic angle. No feedforward or feedback was running during the acquisition to actively stabilize the beam energy. Measured data for the second phase setting, $\theta = -\theta_{\text{magic}}$, are plotted in blue. At this setting, the energy jitter contribution from HV in K01 increases the normalized rms energy jitter to 1.5×10^{-4}.

VI. CONCLUSION AND OUTLOOK

The theory and experimental results verify a correlated shift of the amplitude and phase of accelerating fields caused by HV variations in klystron tubes.

The contribution from HV variations to beam energy and arrival time can be minimized by operating close to the magic angle. Operating the klystrons in saturation minimizes amplitude jitter generated by klystron input signal amplitude noise, which leaves the remaining demands mainly on phase stability in the accelerator, or more precisely, the stability of the low power rf distribution and amplification to feed the klystron tubes.

Linear accelerators used for short-electron-bunch production compress the bunches, usually in several steps. Either in chicane-type compressors, $R_{56} \leq 0$, or in arclike, $R_{56} \geq 0$. The compensation of electron beam energy and timing jitter close to the magic angle can only be implemented for arclike compressors.

The following example indicates the gain of operating at the magic angle. We compare accelerating precrest at a phase angle of −18.5° and compression in a chicane with $R_{56} = -0.0455$ m to acceleration postcrest close to the magic angle at a phase of 18.5° and compression in an arc with $R_{56} = 0.0455$ m. A state-of-the-art HV jitter of 0.002% rms is assumed. The normalized energy and timing jitter were calculated using Eqs. (1) and (6). The result is 1.4×10^{-4} and 21 fs precrest, and for a postcrest phase range, $|\theta - \theta_{\text{magic}}| \leq 1.0°$, the energy jitter is $\leq 4 \times 10^{-6}$ and the timing jitter after the bunch compressor is ≤ 0.6 fs. Allowing the phase to be adjusted ±1° gives tunability of the compression factor between 10 and 1000 for a fixed R_{56}. The HV jitter also affects the compression ratio. In this example, the nominal compression ratio is 18 for both sides of the crest. The calculated compression jitter using Eqs. (8) and (9) is 1.2% at −18.5° and 1.3% at 18.5°. The bunch length jitter is thus comparable but slightly better for precrest acceleration. The contribution from other rf phase and amplitude jitter sources must be added to calculate the total energy, arrival time, and compression jitter. Only modulator HV is included in the example above.

Accelerating phases and electron beam optics (in particular the compressor R_{56}) must be selected and tuned consistently to achieve the desired compression and beam parameters important for the FEL output. Having the magic angle advantage in mind already at the design stage enables parameter choices that make FEL operation fully compatible with running close to the magic angle. Although there are presently no operating FELs driven by linacs with arclike compressors that can benefit from the increased stability offered by operating close to the magic angle, a design for a soft x-ray FEL at MAX IV (SXL) that does operate close to the magic angle was presented in [26].

The Femtomax beamline at MAX IV is used to measure ultrafast processes with hard x-ray photons, produced by spontaneous undulator emission [27]. The beamline science benefits from the increased stability achieved by operating the linac close to the magic angle, with a resulting normalized rms energy jitter of 10^{-4}.

Recent developments at MAX IV show how the measured energy jitter in BC1 is reduced by almost a factor of 2, down to 8.2×10^{-5} by operating at the magic angle. Further research and development aim at reducing the phase jitter well below 0.01° to bring the arrival time jitter toward 1 fs rms, which is comparable to the duration of the short bunches that are simulated for SXL at MAX IV [28].

ACKNOWLEDGMENTS

We would like to thank our colleagues in the accelerator development group at MAX IV, in particular, Francis Cullinan for his review of the manuscript.

[1] S. Li, T. Driver, J. Duris, E. Champenois, J. O'Neal, A. Marinelli, and J. P. Cryan, Attosecond science at x-ray free electron lasers, in *Frontiers in Optics/Laser Science* (Optica Publishing Group, Washington, DC, 2020), p. LW4F.1, 10.1364/LS.2020.LW4F.1.

[2] Z. Geng, P. Craievich, R. Kalt, J. Alex, C. H. Gough, T. Lippuner, M. Pedrozzi, and F. Löhl, RF jitter and electron beam stability in the SwissFEL Linac, in *Proceedings of the 39th Free Electron Laser Conference, Hamburg, Germany* (JACoW, Geneva, Switzerland, 2019), pp. 400–403.

[3] H.-S. Kang, H. Yang, G. Kim, H. Heo, I. Nam, C.-K. Min, C. Kim, S.Youl Baek, H.-J. Choi, G. Mun *et al.*, FEL performance achieved at PAL-XFEL using a three-chicane bunch compression scheme, J. Synchrotron Radiat. **26**, 1127 (2019).

[4] H.-S. Kang, C.-K. Min, H. Heo, C. Kim, H. Yang, G. Kim, I. Nam, S. Y. Baek, H.-J. Choi, G. Mun *et al.*, Hard x-ray free-electron laser with femtosecond-scale timing jitter, Nat. Photonics **11**, 708 (2017).

[5] S. Schulz, M. K, Czwalinna, M. Felber, M. Fenner, C. Gerth, T. Kozak, T. Lamb, B. Lautenschlager, F. Ludwig, U. Mavric *et al.*, Few-femtosecond facility-wide synchronization of the European XFEL, in *Proceedings of the 39th International Free-Electron Laser Conference, Hamburg, Germany* (JACoW, Geneva, Switzerland, 2019).

[6] M. Harmand, R. Coffee, Mina R. Bionta, Matthieu Chollet, D. French, D. Zhu, D. M. Fritz, H. T. Lemke, N. Medvedev, B. Ziaja *et al.*, Achieving few-femtosecond time-sorting at hard x-ray free-electron lasers, Nat. Photonics **7**, 215 (2013).

[7] N. Hartmann, W. Helml, M. R. Bionta, A. Galler, J. Grünert, S. Molodtsov, K. R. Ferguson, S. Schorb, M. L. Swiggers, S. Carron, C. Bostedt, J.-C. Castagna, J. Bozek, J. M. Glownia, D. J. Kane, A. R. Fry, W. E. White, C. P. Hauri, T. Feurer, and R. N. Coffee, Sub-fs precision measurement of relative x-ray arrival time for FELs, in *Proceedings of the 2014 Conference on Lasers and Electro-Optics (CLEO)—Laser Science to Photonic Applications* (Optica Publishing Group, Washington, DC, 2014), pp. 1–2, 10.1364/CLEO_SI.2014.STu3F.6.

[8] S. Schulz, I. Grguraš, C. Behrens, H. Bromberger, J. T. Costello, M. K. Czwalinna, Matthias Felber, M. C. Hoffmann, M. Ilchen, H. Y. Liu *et al.*, Femtosecond all-optical synchronization of an x-ray free-electron laser, Nat. Commun. **6**, 5938 (2015).

[9] Y. Otake, H. Maesaka, S. Matsubara, N. Hosoda, and T. Ohshima, Timing and low-level rf system for an x-ray laser, Phys. Rev. Accel. Beams **19**, 022001 (2016).

[10] S. Hunziker, V. Arsov, F. Buechi, M. Kaiser, A. Romann, V. Schlott, P. Orel, and S. Zorzut, Reference distribution and synchronization system for SwissFEL: Concept and first results, in *Proceedings of IBIC2014, Monterey, CA* (JACoW, Geneva, Switzerland, 2014), MOCZB.

[11] J. S. Oh, T. Hara, T. Inagaki, T. Shintake, and K. Shirasawa, Stable RF phase insensitive to the modulator voltage fluctuation of the C-band main linac for SCSS XFEL, in *Proceedings of the 28th International Free Electron Laser Conference, FEL-2006, Berlin, Germany* (2006), pp. 684–687.

[12] Y. Liu, H. Matsumoto, L. Li, and M. Gu, Analysis the influence of pulse-to-pulse stability of modulator on high-power microwave output of pulsed klystron, SN Appl. Sci. **4**, 4 (2022).

[13] S.-y. Lee, *Accelerator Physics (Fourth Edition)* (World Scientific Publishing Company, Singapore, 2018), ISBN 9789813274686.

[14] P. Emma, Bunch compressor options for the new Tesla parameters, CEA/Saclay Technical Report No. SCAN-9903048, 1998.

[15] R. G. Carter, *Klystrons*, The Cambridge RF and Microwave Engineering Series (Cambridge University Press, Cambridge, England, 2018).

[16] G. S. N. Raju, *Radar Engineering* (I K International Publishing House Pvt. Ltd, New Delhi, 2013), ISBN 9788190694216.

[17] E. G. Cook, Review of solid-state modulators, eConf **C000821**, WE103 (2000), https://accelconf.web.cern.ch/l00/papers/WE103.pdf.

[18] M. N. Nguyen, C. P. Burkhart, B. K. Lam, and B. Morris, Recent upgrade of the klystron modulator at SLAC, in *Proceedings of the 2011 IEEE Pulsed Power Conference, Chicago, IL* (IEEE, New York, 2011), pp. 1386–1391.

[19] H. Hayano, M. Akemoto, T. Naito, S. Takeda, D. Aizawa, M. Higuchi, and T. Sakamoto, Klystron rf stabilization using feedforward circuit, in *Proceedings of the 19th International Linear Accelerators Conference, Chicago, IL, 1998* (NTIS, Springfield, VA, 1998).

[20] A. S. Gilmour, *Klystrons, Traveling Wave Tubes, Magnetrons, Crossed-Field Amplifiers, and Gyrotrons* (Artech House, Norwood, MA, 2011).

[21] S. Di Mitri, Bunch length compressors, CERN Yellow Reports: School Proceedings **1**, 363 (2018).

[22] MAX IV Detailed Design Report. Technical report, MAX-lab, 2010, https://www.maxiv.lu.se/beamlines-accelerators/accelerators/accelerator-documentation-2/.

[23] S. Thorin, J. Andersson, M. Brandin, F. Curbis, L. Isaksson, M. Kotur, F. Lindau, E. Mansten, D. Olsson, R. Svärd, S. Werin, and J. Börklund Svensson, Experience and initial measurements of magnetic linearisation in the MAX IV linac bunch compressors, in *Proceedings of the 38th International Free Electron Laser Conference, FEL2017, Santa Fe, NM* (JACoW, Geneva, Switzerland, 2017), pp. 273–275, 10.18429/JACoW-FEL2017-TUP013.

[24] T. Tiwari and R. Krishnan, Design and development of waveguide type dual directional coupler for s-band linear accelerator, in *Proceedings of the 2008 International Conference on Recent Advances in Microwave Theory and Applications, Jaipur, India* (IEEE, Jaipur, India, 2008), pp. 252–254.

[25] S. Thorin, J. Andersson, F. Curbis, M. Eriksson, O. Karlberg, D. Kumbaro, E. Mansten, D. Olsson, S. Werin *et al.*, The MAX-IV Linac, in *Proceedings of 27th Linear Accelerator*

Conference, LINAC-2014, Geneva, Switzerland (JACoW, Geneva, Switzerland, 2014), pp. 400–403.

[26] The Soft X-Ray Laser @ MAX IV—Conceptual Design Report, MAX-IV Laboratory, Technical report, 2021, https://www.maxiv.lu.se/beamlines-accelerators/accelerators/soft-x-ray-laser/.

[27] H. Enquist, A. Jurgilaitis, A. Jarnac, Å. Bengtsson, M. Burza, F. Curbis, C. Disch, J. C. Ekström, M. Harb, L. Isaksson *et al.*, Femtomax—an x-ray beamline for structural dynamics at the short-pulse facility of MAX IV, J. Synchrotron Radiat. **25**, 570 (2018).

[28] W. Qin, F. Curbis, J. Andersson, V. Goryashko, L. Isaksson, B. Kyle, F. Lindau, E. Mansten, M. Pop, P. Salén, H. Tarawneh, P. F. Tavares, S. Thorin, A. Vorozhtsov, and S. Werin, The FEL in the SXL project at MAX IV, J. Synchrotron Radiat. **28**, 707 (2021).